

# Ab initio calculations of the dynamical response of copper

I. Campillo<sup>1</sup>, A. Rubio<sup>2</sup>, and J. M. Pitarke<sup>1,3</sup>

<sup>1</sup> *Materia Kondentsatuaren Fisika Saila, Zientzi Fakultatea, Euskal Herriko Unibertsitatea, 644 Posta kutxatila, 48080 Bilbo, Basque Country, Spain*

<sup>2</sup> *Departamento de Física Teórica, Universidad de Valladolid, E-47011 Valladolid, Spain*

<sup>3</sup> *Donostia International Physics Center (DIPC) and Centro Mixto CSIC-UPV/EHU (October 14, 2018)*

The role of localized  $d$ -bands in the dynamical response of Cu is investigated, on the basis of *ab initio* pseudopotential calculations. The density-response function is evaluated in both the random-phase approximation (RPA) and a time-dependent local-density functional approximation (TDLDA). Our results indicate that in addition to providing a polarizable background which lowers the free-electron plasma frequency,  $d$ -electrons are responsible, at higher energies and small momenta, for a double-peak structure in the dynamical structure factor. These results are in agreement with the experimentally determined optical response of copper. We also analyze the dependence of dynamical scattering cross sections on the momentum transfer.

PACS numbers: 71.45.Gm, 72.30.+q, 78.20.-e, 78.70.Ck

Noble-metal systems have been the focus of much experimental and theoretical work in order to get a better understanding of how electronic properties of delocalized, free-electron-like, electrons are altered by the presence of localized  $d$ -electrons. Silver is one of the best understood systems, where the free-electron plasma frequency is strongly renormalized (red-shifted) by the presence of a polarizable background of  $d$ -electrons<sup>1</sup>. Unlike silver, copper presents no decoupling between  $sp$  and  $d$  orbitals, and a combined description of these one-electron states is needed to address both structural and electronic properties of this material. Though in the case of other materials, as semiconductors, electron-hole interactions (excitonic renormalization) strongly modify the single-particle optical absorption profile<sup>2</sup>, metals offer a valuable playground for investigations of dynamical exchange-correlation effects of interacting many-electron systems within a quasiparticle picture<sup>3</sup>. Indeed, *ab initio* calculations of the dynamical response of a variety of simple metals, as obtained within the random-phase-approximation (RPA), successfully account for the experimentally determined plasmon dispersion relations<sup>4</sup> and scattering cross sections<sup>5</sup>. Within the same many-body framework, *ab initio* calculations of the electronic stopping power of real solids have also been reported<sup>6</sup>.

Since the pioneering investigations by Ehrenreich and Philipp<sup>7</sup> on the optical absorption and reflectivity of Ag and Cu, a variety of measurements of the optical properties of copper has been reported<sup>8</sup>. Nevertheless, there have been, to the best of our knowledge, no first-principles calculations of the dielectric response function of Cu that include the full effects of the crystal lattice. Furthermore, the dynamical density-response function is well-known to be a key quantity in discussing one-electron properties in real metals, and it is also of basic importance in the description of low-dimensional copper systems studied in optical and time-resolved femtosecond experiments<sup>9,10</sup>.

In this Rapid Communication we report a first-

principles evaluation of the dynamical density-response function of Cu, as computed in the RPA and a time-dependent extension of local-density functional theory (TDLDA), after an expansion of  $4s^1$  and  $3d^{10}$  one-electron Bloch states in a plane-wave basis with a kinetic-energy cutoff of 75 Ry<sup>11</sup>. Though all-electron mixed basis schemes, such as the full-potential linearized augmented plane wave (LAPW) method<sup>12</sup>, are expected to be well suited for the description of the response of localized  $d$ -electrons, plane-wave pseudopotential approaches offer a simple and well-defined scenario to describe ground-state properties and dynamical response functions<sup>13</sup>. This approach has already been successfully incorporated in the description of inelastic lifetimes of excited electrons in copper<sup>14</sup>, and could also be applied to the study of other noble and transition metals.

The key quantity in our calculations is the dynamical density-response function  $\chi(\mathbf{r}, \mathbf{r}'; \omega)$ . For periodic crystals we Fourier transform this function into a matrix  $\chi_{\mathbf{G}, \mathbf{G}'}(\mathbf{q}, \omega)$  which, in the framework of time-dependent density-functional theory (DFT)<sup>15,16</sup>, satisfies the matrix equation

$$\chi_{\mathbf{G}, \mathbf{G}'}(\mathbf{q}, \omega) = \chi_{\mathbf{G}, \mathbf{G}'}^0(\mathbf{q}, \omega) + \sum_{\mathbf{G}''} \sum_{\mathbf{G}'''} \chi_{\mathbf{G}, \mathbf{G}''}^0(\mathbf{q}, \omega) \times [v_{\mathbf{G}''}(\mathbf{q}) \delta_{\mathbf{G}'', \mathbf{G}'''} + K_{\mathbf{G}'', \mathbf{G}'''}^{xc}(\mathbf{q}, \omega)] \chi_{\mathbf{G}''', \mathbf{G}'}(\mathbf{q}, \omega). \quad (1)$$

Here, the wave vector  $\mathbf{q}$  is in the first Brillouin zone (BZ),  $\mathbf{G}$  and  $\mathbf{G}'$  are reciprocal lattice vectors,  $v_{\mathbf{G}}(\mathbf{q}) = 4\pi/|\mathbf{q} + \mathbf{G}|^2$  are the Fourier coefficients of the bare Coulomb potential, the kernel  $K_{\mathbf{G}, \mathbf{G}'}^{xc}(\mathbf{q}, \omega)$  accounts for short-range exchange-correlation effects<sup>16</sup>, and  $\chi_{\mathbf{G}, \mathbf{G}'}^0(\mathbf{q}, \omega)$  are the Fourier coefficients of the density-response function of noninteracting Kohn-Sham electrons:

$$\chi_{\mathbf{G}, \mathbf{G}'}^0(\mathbf{q}, \omega) = \frac{1}{\Omega} \sum_{\mathbf{k}} \sum_{n, n'}^{BZ} \frac{f_{\mathbf{k}, n} - f_{\mathbf{k} + \mathbf{q}, n'}}{E_{\mathbf{k}, n} - E_{\mathbf{k} + \mathbf{q}, n'} + \hbar(\omega + i\eta)} \times \langle \phi_{\mathbf{k}, n} | e^{-i(\mathbf{q} + \mathbf{G}) \cdot \mathbf{r}} | \phi_{\mathbf{k} + \mathbf{q}, n'} \rangle \langle \phi_{\mathbf{k} + \mathbf{q}, n'} | e^{i(\mathbf{q} + \mathbf{G}') \cdot \mathbf{r}} | \phi_{\mathbf{k}, n} \rangle, \quad (2)$$

where the second sum runs over the band structure for each wave vector  $\mathbf{k}$  in the first BZ,  $f_{\mathbf{k},n}$  are Fermi factors,  $\eta$  is a positive infinitesimal<sup>17</sup>, and  $\Omega$  represents the normalization volume. The one-particle Bloch states  $\phi_{\mathbf{k},n}(\mathbf{r},\omega)$  and energies  $E_{\mathbf{k},n}$  are the self-consistent eigenfunctions and eigenvalues of the Kohn-Sham equations of DFT<sup>15</sup>, which we solve within the so-called local-density approximation (LDA)<sup>18</sup> for exchange and correlation effects. The electron-ion interaction is described by a non-local, norm-conserving, ionic pseudopotential<sup>20</sup> in a non-separable form, so as to have a better description of the conduction bands entering Eq. (2).

The calculations presented below have been found to be well converged for all frequencies and wave vectors under study, and they have been performed by including conduction bands up to a maximum energy of 80 eV above the Fermi level. BZ integrations were performed by sampling on a  $10 \times 10 \times 10$  Monkhorst-Pack mesh<sup>19</sup>. In the RPA the kernel  $K_{\mathbf{G},\mathbf{G}'}^{xc}(\mathbf{q},\omega)$  is taken to be zero. In the TDLDA the zero-frequency kernel, approximated within the LDA by a contact delta function, is adiabatically extended to finite frequencies<sup>16,21</sup>. In both RPA and TDLDA, crystalline local field effects appearing through the dependence of the diagonal elements of the interacting response matrix  $\chi_{\mathbf{G},\mathbf{G}'}(\mathbf{q},\omega)$  on the off-diagonal elements of the polarizability  $\chi_{\mathbf{G},\mathbf{G}'}^0(\mathbf{q},\omega)$  have been fully included in our calculations<sup>22</sup>.

The properties of the long-wavelength limit ( $\mathbf{q} \rightarrow 0$ ) of the dynamical density-response function are accessible by measurements of the optical absorption, through the imaginary part of the dielectric response function  $\epsilon_{\mathbf{G}=0,\mathbf{G}'=0}(\mathbf{q}=0,\omega)$ . On the other hand, the scattering cross-section for inelastic scattering of either X-rays or fast electrons with finite momentum transfer  $\mathbf{q} + \mathbf{G}$  is, within the first Born approximation, proportional to the dynamical structure factor

$$S(\mathbf{q} + \mathbf{G}, \omega) = \frac{2}{v_{\mathbf{G}}(\mathbf{q})} \text{Im} \left[ -\epsilon_{\mathbf{G},\mathbf{G}}^{-1}(\mathbf{q}, \omega) \right], \quad (3)$$

where

$$\epsilon_{\mathbf{G},\mathbf{G}'}^{-1}(\mathbf{q}, \omega) = \delta_{\mathbf{G},\mathbf{G}'} + v_{\mathbf{G}'}(\mathbf{q}) \chi_{\mathbf{G},\mathbf{G}'}(\mathbf{q}, \omega). \quad (4)$$

Fig. 1 exhibits, by solid lines, our results for both real and imaginary parts of the  $\epsilon_{\mathbf{G},\mathbf{G}}(\mathbf{q},\omega)$  dielectric function of copper, for a small momentum transfer of  $|\mathbf{q} + \mathbf{G}| = 0.18 a_0^{-1}$  ( $a_0$  is the Bohr radius), together with the optical data ( $\mathbf{q} = 0$ ) of Ref. 8 (dashed lines). In this low- $\mathbf{q}$  limit, both RPA and TDLDA dynamical density-response functions coincide, and the dielectric function is obtained from the dynamical density-response function of noninteracting Kohn-Sham electrons<sup>3</sup>. Corresponding values of the so-called energy-loss function  $\text{Im} \left[ -\epsilon_{\mathbf{G},\mathbf{G}}^{-1}(\mathbf{q}, \omega) \right]$  are presented in Fig. 2, and a comparison between the imaginary parts of interacting  $\chi_{\mathbf{G},\mathbf{G}}(\mathbf{q},\omega)$  and noninteracting  $\chi_{\mathbf{G},\mathbf{G}}^0(\mathbf{q},\omega)$  density-response functions is displayed in the inset of this figure, showing that as the Coulomb

interaction is turned on the oscillator strength is redistributed. Our results, as obtained for a small but finite momentum transfer, are in excellent agreement with the experimentally determined dielectric function, both showing a double peak structure in  $\text{Im} \left[ -\epsilon_{\mathbf{G},\mathbf{G}}^{-1}(\mathbf{q}, \omega) \right]$ .

In order to investigate the role of localized  $d$ -bands in the dynamical response of copper, we have also used an *ab initio* pseudopotential with the  $3d$  shell assigned to the core. The result of this calculation, displayed in Fig. 2 by a dotted line, shows that a combined description of both localized  $3d^{10}$  and delocalized  $4s^1$  electrons is needed to address the actual electronic response of copper. On the one hand, the role played in the long-wavelength limit by the Cu  $d$ -bands is to provide a polarizable background which lowers the free-electron plasma frequency by  $\sim 2.5$  eV<sup>23</sup>. We note from Fig. 1 that near 8.5 eV the real part of the dielectric function ( $\text{Re} \epsilon$ ) is zero; however, the imaginary part ( $\text{Im} \epsilon$ ) is not small, due to the existence of interband transitions at these energies which completely damp the free-electron plasmon. On the other hand,  $d$ -bands are also responsible, at higher energies, for a double-peak structure in the energy-loss function, which stems from a combination of band-structure effects and the building up of collective modes of  $d$ -electrons. Since these peaks occur at energies ( $\sim 20$  eV and  $\sim 30$  eV) where  $\text{Re} \epsilon$  is nearly zero (see Fig. 1), they are in the nature of collective excitations, the small but finite value of  $\text{Im} \epsilon$  at these energies accounting for the width of the peaks.

A better insight onto the origin of the double-hump in the energy-loss function is achieved from Fig. 3, where the density of states (DOS) and the joint-density of states (J-DOS) of Cu are plotted. The high-energy peak present in the J-DOS spectrum at about 25 eV, which appears as a result of transitions between  $d$ -bands at  $\sim 2$  eV below the Fermi level and unoccupied states with energies of  $\sim 23$  eV above the Fermi level, is responsible for the peak of electron-hole excitations in  $\text{Im} \epsilon$  and  $\text{Im} \chi^0$  at  $\omega = 25$  eV (see Fig. 1 and the inset of Fig. 2). Hence, there is a combination, at high energies, of  $d$ -like collective excitations and interband electron-hole transitions, which results in a prominent double-peak in the loss spectrum.

Now we focus on the dependence of the energy-loss function on the momentum transfer  $\mathbf{q} + \mathbf{G}$ . As long as the  $3d$  shell of Cu is assigned to the core, we find a well-defined free-electron plasmon for wave vectors up to the critical momentum transfer where the plasmon excitation enters the continuum of intraband particle-hole excitations. This free-electron plasmon, which shows a characteristic positive dispersion with wave vector, is found to be completely damped when a realistic description of  $3d$  orbitals is included in the calculations. At higher energies and small momenta,  $d$ -like collective excitations originate a double-peak structure which presents no dispersion, as shown in Fig. 4. In this figure the RPA dynamical structure factor for  $\mathbf{G} = 0$  is displayed, as obtained for various

values of  $q$  along the (100) direction. For larger values of the momentum transfer  $\mathbf{q} + \mathbf{G}$ , single-particle excitations take over the collective ones up to the point that above a given cutoff the spectra is completely dominated by the kinetic-energy term<sup>3,10</sup>.

In Fig. 5 we show the computed dynamical structure factor for  $|\mathbf{q} + \mathbf{G}| = 1.91a_0^{-1}$  along the (111) direction, in both RPA (solid line) and TDLDA (dashed line), together with the result of replacing the interacting  $\chi_{\mathbf{G},\mathbf{G}}(\mathbf{q},\omega)$  matrix by its noninteracting counterpart  $\chi_{\mathbf{G},\mathbf{G}}^0(\mathbf{q},\omega)$  (dotted line). The noninteracting dynamical structure factor (dotted line) now reproduces the main features of full RPA and TDLDA calculations. The double peak of Fig. 2, which is in the nature of plasmons, is now replaced by a less pronounced double-hump originated from single electron-hole excitations. A similar double-peak has been found in the loss spectra of simple metals<sup>5</sup>, which has been understood on the basis of the existence of a gap region for interband transitions<sup>24</sup>. We also note that the effect of short-range exchange-correlation effects, which are absent in the RPA, is to reduce the effective electron-electron interaction, thus the dynamical structure factor being closer in TDLDA than in RPA from the result obtained for noninteracting Kohn-Sham electrons. The RPA dynamical structure factor of Cu is enhanced by up to a 40% by the inclusion, within the TDLDA, of many-body local field corrections.

In summary, we have presented *ab initio* pseudopotential calculations of the dynamical density-response function of Cu, by including  $d$ -electrons as part of the valence complex. In the long-wavelength limit ( $\mathbf{q} \rightarrow 0$ ),  $d$ -bands provide a polarizable background that lowers the free-electron plasma frequency.  $d$ -electrons are also responsible for a full damping of this  $s$ -like collective excitation and for the appearance of a  $d$ -like double-peak structure in the energy-loss function, in agreement with the experimentally determined optical response of copper. We have analyzed the dependence of the dynamical structure factor on the momentum transfer, and we have found that, for values of the momentum transfer over the cutoff wave vector for which collective excitations enter the continuum of intraband electron-hole pairs, a less-pronounced double-hump is originated by the existence of interband electron-hole excitations. Experimental measurements of scattering cross sections in Cu would be desirable for the investigation of many-body effects, which we have approximated within RPA and TDLDA.

We thank P. M. Echenique for stimulating discussions. I.C. and J.M.P. acknowledge partial support by the Basque Unibertsitate eta Ikerketa Saila and the Spanish Ministerio de Educación y Cultura. A.R. acknowledges the hospitality of the Departamento de Física de Materiales, Universidad del País Vasco, San Sebastián, where part of this work was carried out.

- <sup>1</sup> E. Zaremba and K. Sturm, Phys. Rev. Lett. **55**, 750 (1985); A. Liebsch, Phys. Rev. Lett. **71**, 145 (1993); Ll. Serra and A. Rubio, Phys. Rev. Lett. **78**, 1428 (1997)
- <sup>2</sup> M. Rohlfing and S. G. Louie, Phys. Rev. Lett. **81**, 2312 (1998); L. X. Benedict *et al*, Phys. Rev. Lett. **80**, 4514 (1998); S. Albrecht *et al*, Phys. Rev. Lett. **80**, 4510 (1998).
- <sup>3</sup> D. Pines and P. Nozieres, *The Theory of Quantum Liquids, Volume I: Normal Fermi Liquids*, (Addison-Wesley, New York 1989).
- <sup>4</sup> A. A. Quong and A. G. Eguiluz, Phys. Rev Lett. **70**, 3955 (1993); F. Aryasetiawan and K. Karlsson, Phys. Rev. Lett. **73**, 1679 (1994); A. Fleszar *et al*, Phys. Rev. B **55**, 2068 (1997).
- <sup>5</sup> N. E. Maddocks *et al*, Europhys. Lett. **27**, 681 (1994); Phys. Rev. B **49**, 8502 (1994); A. Fleszar *et al*, Phys. Rev. Lett. **74**, 590 (1995).
- <sup>6</sup> I. Campillo *et al*, Phys. Rev. B **58**, 10307 (1998); Nucl. Instrum. Methods B **135**, 103 (1998).
- <sup>7</sup> H. Ehrenreich and H. R. Philipp, Phys. Rev. **128**, 1622, (1962).
- <sup>8</sup> E.D. Palik, *Handbook of Optical Constants of Solids* (Academic press, New York, 1985).
- <sup>9</sup> T.V. Shahbazyan *et al*, Phys. Rev. Lett. **81**, 3120 (1998).
- <sup>10</sup> A. Rubio *et al*, Int. J. Mod. Phys. B **11**, 2727 (1997).
- <sup>11</sup> This cutoff corresponds to keeping approximately 900  $\mathbf{G}$  vectors in the plane-wave expansion.
- <sup>12</sup> D. J. Singh, *Plane Waves, Pseudopotentials, and the LAPW Method* (Kluwer, Boston, 1994).
- <sup>13</sup> W. E. Pickett, Comput. Phys. Reports **9**, 115 (1989); M. C. Payne *et al*, Rev. Mod. Phys. **64**, 1045 (1992).
- <sup>14</sup> I. Campillo, J. M. Pitarke, A. Rubio, E. Zarate, and P. M. Echenique, to be published.
- <sup>15</sup> P. Hohenberg and W. Kohn, Phys. Rev. **136**, B864 (1964); W. Kohn and L. Sham, Phys. Rev. **140**, A1133 (1965).
- <sup>16</sup> M. Petersilka *et al*, Phys. Rev. Lett. **76**, 1212 (1996).
- <sup>17</sup> An important issue is the role of the numerical damping,  $\eta$ , introduced in the evaluation of Eq. (2). We have performed calculations with three different values of  $\eta$ : 0.1, 0.2 and 0.4 eV, and we have found no differences apart from some noise at 0.1 and 0.2 eV.
- <sup>18</sup> D. M. Ceperley and B. J. Alder, Phys. Rev. Lett. **45**, 1196 (1980), as parametrized by J. P. Perdew and A. Zunger, Phys. Rev. B **23**, 5048 (1981).
- <sup>19</sup> H. J. Monkhorst and J. D. Pack, Phys. Rev. B **13**, 5188 (1976).
- <sup>20</sup> N. Troullier and J. L. Martins, Phys. Rev. B **43**, 1993 (1991). The pseudopotential for Cu reproduces within a few percent all the structural properties of this material.
- <sup>21</sup> A. Zangwill and P. Soven, Phys. Rev. A **21**, 1561 (1980).
- <sup>22</sup> We have also solved Eq. (1) with all off-diagonal elements of the polarizability excluded, and we have found quantitative deviations from the full calculations of about 10-20% for energies above 30 eV. Calculations, as obtained with inclusion of local-field effects, have been performed with use of 15  $\mathbf{G}$ , 27  $\mathbf{G}$  and 89  $\mathbf{G}$  vectors in Eq. (1), and the results presented here have been found to be well converged, for all values of the wave vector  $\mathbf{q}$  used in our calculations, with 15  $\mathbf{G}$  vectors in the representation of the matrix  $\chi_{\mathbf{G},\mathbf{G}'}^0$ .
- <sup>23</sup> The plasma frequency of a free-electron gas with the electron density equal to that of valence ( $4s^1$ ) electrons in Cu

is  $\omega_p = 10.8 \text{ eV}$ .

<sup>24</sup> In the case of Cu, there exists an excitation gap in the L-point of the BZ for energies between 20 eV and 30 eV above the Fermi level.

FIG. 1. Real and imaginary parts of the  $\epsilon_{\mathbf{G},\mathbf{G}}(\mathbf{q},\omega)$  dielectric function of Cu, for  $\mathbf{q} = 0.2(1, 0, 0) \times (2\pi)/a$  ( $a = 3.61 \text{ \AA}$  is the experimental lattice constant) and  $\mathbf{G} = 0$ . Solid and dashed lines represent our calculations and the optical data of Ref. 8, respectively.

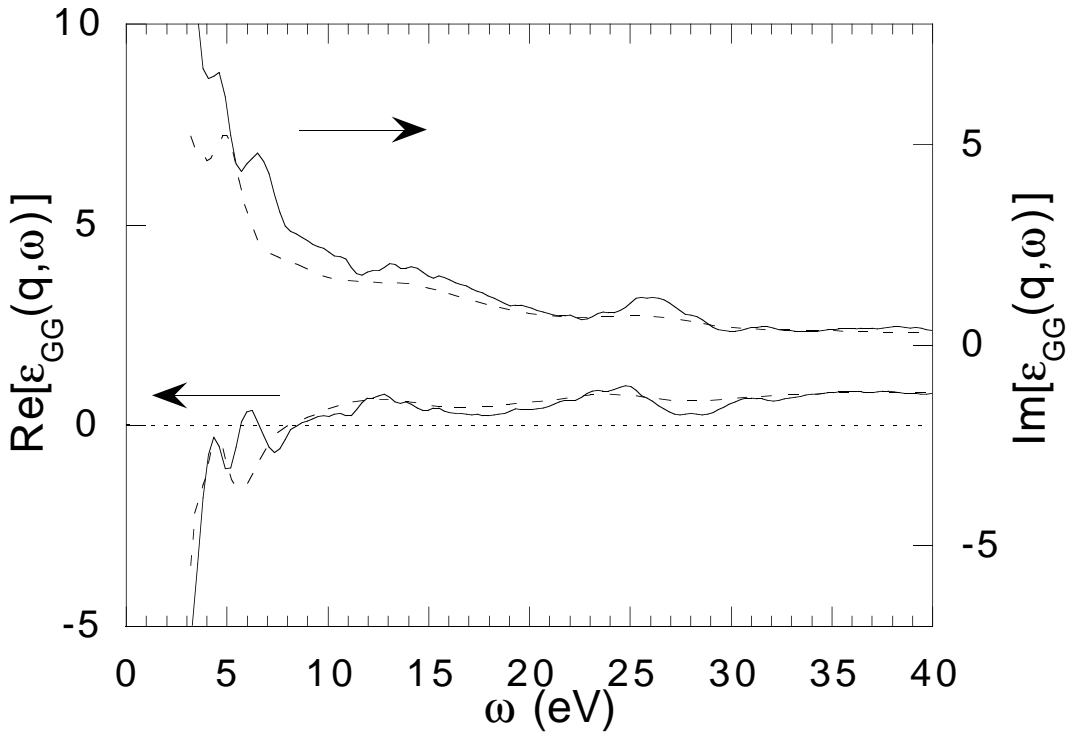
FIG. 2. As in Fig. 1, for the energy-loss function of Cu. The dotted line represents the result of assigning the  $3d$  shell to the core. In the inset the imaginary parts of interacting (solid line) and noninteracting (dashed line) density-response functions are compared, for the same values of  $\mathbf{q}$  and  $\mathbf{G}$ .

FIG. 3. Calculated Density of States (DOS) and Joint-Density of States (J-DOS) of Cu. The 25 eV peak in the J-DOS mainly corresponds to transitions from the  $d$  band to unoccupied states with energies of  $\sim 23 \text{ eV}$  above the Fermi level. The J-DOS is a first order approximation to the optical spectra, when matrix-element renormalization and Coulomb interactions are neglected. The DOS and the J-DOS were computed using an interpolation scheme based on the linear tetrahedron method with a  $20 \times 20$  Monkhorst-Pack mesh.

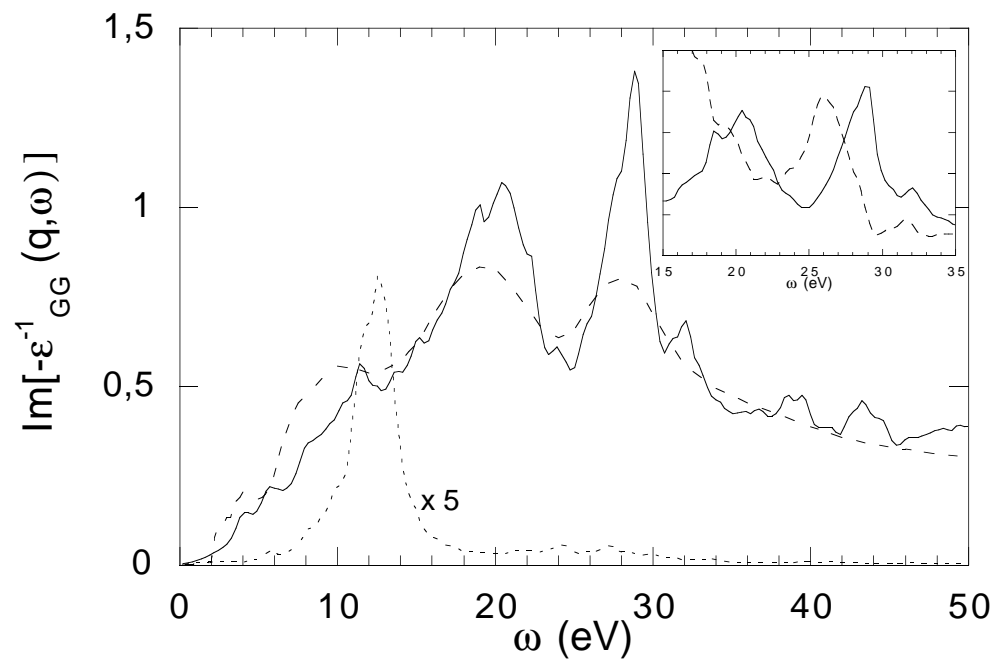
FIG. 4. RPA energy-loss function of Cu along the (100) direction, for various values of the momentum transfer  $|\mathbf{q}+\mathbf{G}|$ : 0.2, 0.4 and 0.8, in units of  $2\pi/a$  ( $a = 3.61 \text{ \AA}$ ).

FIG. 5. RPA (solid line) and TDLDA (dashed line) dynamical structure factors of copper, for  $|\mathbf{q} + \mathbf{G}| = 1.91a_0^{-1}$  along the (111) direction ( $\mathbf{q} = 0.2(1, 1, 1) \times (2\pi/a)$  and  $\mathbf{G} = (1, 1, 1) \times (2\pi/a)$ ). The dotted line represents the result of replacing the interacting density-response matrix by its noninteracting counterpart.

Figure 1



**Figure 2**



**Figure 3**

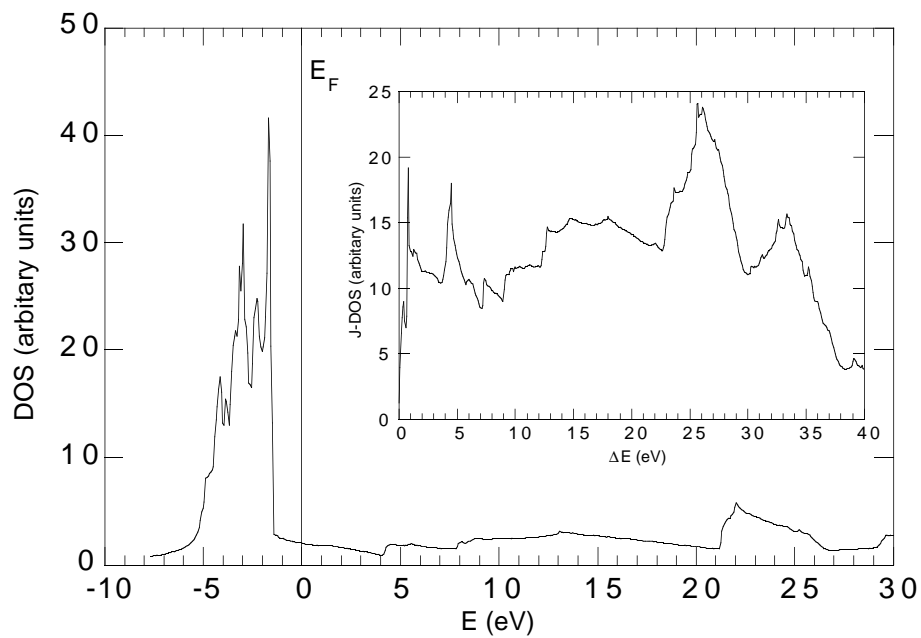


**Figure 4**

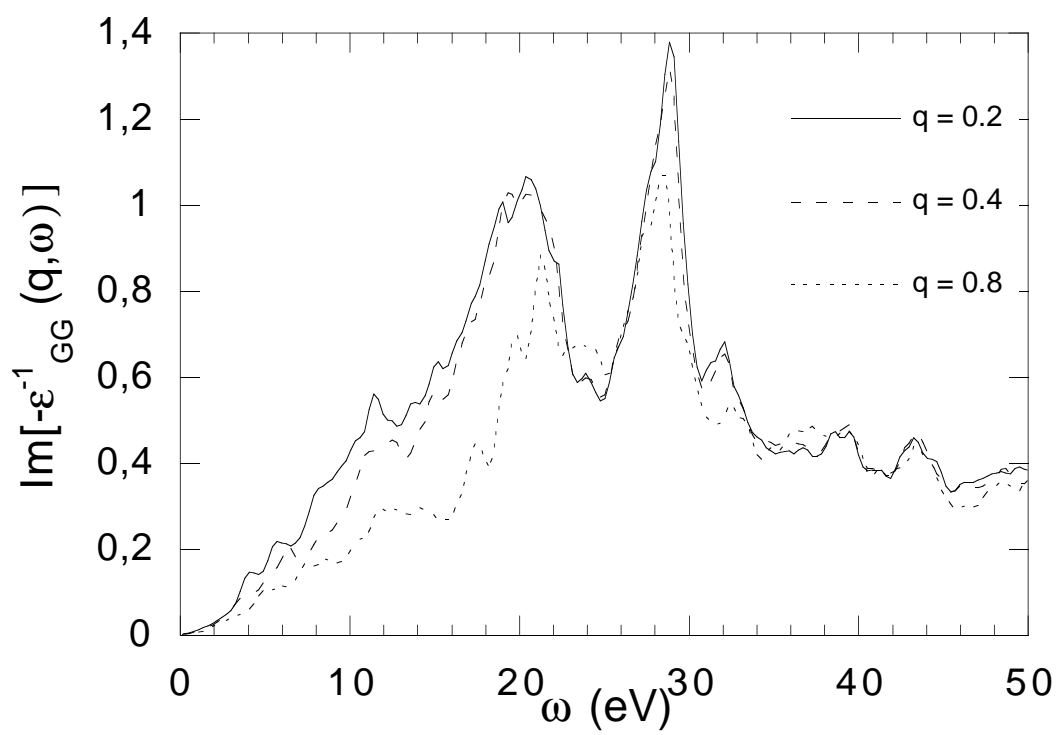




**Figure 5**

